Lyapunov spectrum and synchronization of piecewise linear map lattices with power-law coupling

Antônio M. Batista,* Sandro E. de S. Pinto, Ricardo L. Viana, and Sergio R. Lopes
Departamento de Física, Universidade Federal do Paraná, 81531-990 Curitiba, Paraná, Brazil
(Received 10 August 2001; published 2 May 2002)

We study the synchronization properties of a lattice of chaotic piecewise linear maps. The coupling strength decreases with the lattice distance in a power-law fashion. We obtain the Lyapunov spectrum of the coupled map lattice and investigate the relation between spatiotemporal chaos and synchronization of amplitudes and phases, using suitable numerical diagnostics.

DOI: 10.1103/PhysRevE.65.056209 PACS number(s): 05.45.−a

I. INTRODUCTION

Coupled map lattices are spatially extended dynamical systems suitable to illustrate the interplay of spatial and temporal degrees of freedom and the phenomena resulting from this synergy as domain formation, traveling waves, spatiotemporal intermittency, defect propagation, and fully developed turbulence [1,2]. One of the most intensively studied collective phenomena in spatially extended system is synchronization [3]. While synchronization of periodic system is a well-known subject with a venerable history, for chaotic systems this investigation is relatively new [4].

The diversity of dynamical phenomena exhibited by lattices of coupled chaotic maps can be revealed by describing the various types of synchronized regimes they display. The question of how synchronization and chaos are related in coupled map lattices and oscillator chains has received a great deal of attention in recent years [5]. In this paper, we focus on the influence of the coupling between maps on the amplitude and phase-synchronization properties, as well as on the corresponding Lyapunov spectrum.

The effective coupling range is a key factor to determine whether or not the maps mutually synchronize. Short range (nearest-neighbor or diffusive) couplings do not favor synchronization, since the coupling effect is typically too weak to overcome the disorder caused by the map dynamics [6,7]. On the other hand, nonlocal couplings tend to facilitate synchronization, since the coupling effect extends throughout the lattice, as in globally coupled map lattices, where each site interacts with the mean field produced by all the other ones [8,9]. Nonlocal couplings appear in neural network architectures with local production of information [10], and also result from discretization of some partial integro-differential equations modeling physico-chemical reactions [11]. Further applications of nonlocal couplings are in assemblies of biological cells with oscillatory activity, whose interaction is mediated by some rapidly diffusing chemical substance [12], and in systems of diffusion coupling in nucleation kinetics, with elimination of the rapidly diffusing components [13].

We consider a form of coupling whose intensity decays with the distance along the lattice in a power-law fashion. Such power-law coupling have been used in models of some biological neural networks [14]. Other nonlocal couplings of interest are intermediate range couplings, that consider a finite number of non-nearest neighbors [15]; and small-world networks, which have regular couplings with nearest and non-nearest neighbors as well as a small number of randomly chosen nonlocal interactions [16]. The power-law coupling to be considered in this paper presents an effective range parameter, in such a way that we are able to pass continuously from a local to a global coupling scheme. It was used for studies of an extended Kuramoto model [17], chains of coupled kicked limit-cycle oscillators [18], coupled sine-circle map lattices [19], and coupled van der Pol oscillators [20]. The synchronization properties of these systems were found to be strongly dependent on the effective range, and there occurs a nonequilibrium phase transition [21] between a synchronized and a nonsynchronized state as we go from a global to a local coupling form [19,20].

In this paper, we analyze a lattice of chaotic piecewise linear maps, so as to investigate the effects of a varying coupling range on the number of positive Lyapunov exponents of the system. The Lyapunov spectrum in the local coupling case has been studied by Kaneko [7], and by Isola *et al.* [22], who stressed its connection with the spectrum of the discrete Schrödinger operator in quantum mechanics [23]. The corresponding spectrum for globally coupled lattices was also considered by Kaneko [8]. We study the Lyapunov spectrum by means of the corresponding Kolmogorov-Sinai (KS) entropy [24] and Lyapunov dimension [25]. The former may be used to build a thermodynamical formalism for coupled map lattices [26]. We have previously investigated the effect of a variable effective range for a lattice of coupled logistic maps at a crisis [27].

Another issue to be addressed in this paper is the synchronization properties of the coupled map lattice and their relations with its Lyapunov spectrum. For describing amplitude (or complete) synchronization we have used as numerical diagnostics the space-averaged amplitude and its dispersion, and a complex-valued order parameter [28]. According to the phase definition of Hu and Liu [29], we also characterized phase-synchronized states.

This paper is organized as follows: in Sec. II we study the Lyapunov spectrum, and Sec. III is devoted to an investigation of the amplitude synchronization. Phase synchronization

*Permanent address: Departamento de Matemática e Estatística, Universidade Estadual de Ponta Grossa, 84033-240, Ponta Grossa, Paraná, Brazil.

is considered in Sec. IV, and the Sec. V contains our conclusions.

II. LYAPUNOV SPECTRUM

We examine a lattice of N coupled piecewise linear maps $x \mapsto f(x) = \beta x \pmod 1$, where $x_n^{(i)} \in [0,1)$ represents the state variable for the site i ($i = 1,2,\ldots,N$) at time n, and $\beta > 1$. A power-law coupling is given by [19]

$$x_{n+1}^{(i)} = (1-\epsilon) f(x_n^{(i)}) + \frac{\epsilon}{\eta(\alpha)} \sum_{j=1}^{N'} \frac{1}{j^\alpha} [f(x_n^{(i+j)}) + f(x_n^{(i-j)})], \tag{1}$$

where $\epsilon > 0$ and $\alpha > 0$ are the coupling strength and range, respectively, and

$$\eta(\alpha) = 2 \sum_{j=1}^{N'} \frac{1}{j^\alpha} \tag{2}$$

is a normalization factor, with $N' = (N-1)/2$ for N odd.

The coupling term in Eq. (1) is a weighted average of discretized second spatial derivatives, the normalization factor being the sum of the corresponding weights. If $\alpha \to \infty$, only those terms with $j = 1$ will contribute to the summations present in the coupling term, which results in $\eta \to 2$, so that we obtain the usual future Laplacian coupling

$$x_{n+1}^{(i)} = (1-\epsilon) f(x_n^{(i)}) + \frac{\epsilon}{2} [f(x_n^{(i+1)}) + f(x_n^{(i-1)})], \tag{3}$$

which connects nearest neighbors only [1,6]. In the case where $\alpha = 0$, we have that $\eta = N-1$ and the coupling becomes of a global type

$$x_{n+1}^{(i)} = (1-\epsilon) f(x_n^{(i)}) + \frac{\epsilon}{N-1} \sum_{j=1, j \neq i}^{N} f(x_n^{(j)}), \tag{4}$$

where each site interacts with the mean value of all lattice sites, irrespective of their relative positions (''mean-field'' model) [8]. The power-law coupling in Eq. (1) may be regarded as a kind of interpolating form between these limiting cases. Further properties of the coupling term for arbitrary α may be found in Ref. [18].

The (uncoupled) piecewise linear map $f(x) = \beta x \pmod 1$ has Lyapunov exponent $\lambda_U = \ln \beta$ for almost all initial conditions x_0 (except a Lebesgue measure zero set of points where the map is discontinuous), such that for $\beta > 1$ we have a strongly chaotic dynamics. On the other hand, the coupled map lattice (1) exhibits a Lyapunov spectrum consisting of N ordered exponents $\lambda_1 = \lambda_{max} > \lambda_2 > \cdots > \lambda_N$. For the two limiting cases of the coupling prescription (1) this spectrum is analytically known thanks to the constant slope of $f(x)$. For $\alpha \to \infty$ we have the local or diffusive coupling (3). Using periodic boundary conditions, $x_n^{(0)} = x_n^{(N)}$, the Jacobian matrices are symmetric and circulant, and the corresponding Lyapunov spectrum is [7,22,30]

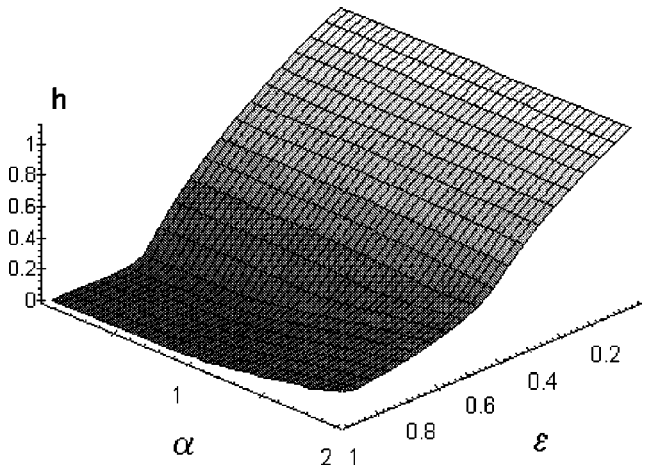

FIG. 1. KS- entropy density in terms of the coupling range and strength, for a lattice of $N = 501$ piecewise linear maps with $\beta = 3.0$, periodic boundary conditions and random initial conditions.

$$\lambda_j(\beta,\epsilon) = \ln \beta + \ln \left| 1 - \epsilon \left[1 - \cos\left(\frac{2\pi j}{N} \right) \right] \right|$$

$$(j = 1,2,\ldots,N). \tag{5}$$

Likewise, for $\alpha = 0$ the global *mean-field* coupling in Eq. (4) leads to the following $(N-1)$-fold degenerate Lyapunov spectrum [8]

$$\lambda_1(\beta) = \ln \beta, \tag{6}$$

$$\lambda_j(\beta,\epsilon) = \ln \left| \beta \left[1 - \epsilon \left(1 + \frac{1}{N-1} \right) \right] \right| \quad (j = 2,3,\ldots,N),$$

provided $\epsilon < (N-1)/N$.

In a coupled map lattice it may well happen that many exponents are positive, hence a quantity of interest is the density of KS entropy [31,32]

$$h = \langle \lambda_j \rangle_{j, \lambda_j > 0} = \frac{1}{N} \sum_{j=1}^{\lambda_j > 0} \lambda_j . \tag{7}$$

It must be stressed that the equality between h and the density of KS entropy holds rigorously for systems having a Sinai-Ruelle-Bowen (SRB) measure [23]. SRB measures were constructed for certain coupled map lattices [33].

We analyze the dependence of the KS-entropy density with the power-law coupling strength ϵ and effective range α. Figure 1 shows a plot of h *versus* α and ϵ for a lattice of piecewise linear maps with $\beta = 3$. For a global coupling ($\alpha = 0$) the mean value of the KS-entropy density is close to zero for strong coupling (large ϵ) and at a given critical value $\epsilon^* \approx 0.6$ it grows monotonically to a maximum value, achieved for vanishing coupling, and turns to be just the Lyapunov exponent for uncoupled maps $\lambda_U = \ln 3 \approx 1.098$.

It is possible to understand this transition based on the Lyapunov spectrum for the global coupling case given by Eq. (6). Except for $\lambda_1 = \ln \beta$, which is always positive for $\beta > 1$, the other $N-1$ exponents are positive provided ϵ

$<\epsilon_c=1-(1/\beta)$. Hence, for $\epsilon \geqslant \epsilon_c$ the KS-entropy density is typically very small and actually vanishes for $N\to\infty$. For $0<\epsilon<\epsilon_c$ all the exponents are positive, and the KS-entropy density depends on ϵ as

$$h(\beta,\epsilon;\alpha=0)=\frac{1}{N}\left\{\ln\beta+(N-1)\ln\left[\beta\left(1-\epsilon-\frac{\epsilon}{N-1}\right)\right]\right\}. \tag{8}$$

For $\beta=3$ and large N, h goes to zero for $\epsilon\geqslant\epsilon_c=2/3$, in agreement with the result depicted in Fig. 1.

As the effective range increases, we still have such a transition for some critical coupling strength $\epsilon^*(\alpha)$, after which the KS-entropy density builds up and achieves its maximum value λ_U when the maps are uncoupled. For stronger coupling (higher ϵ) the KS-entropy density has a positive value that increases with α. When α is large the coupling between maps becomes effectively noticeable with nearest neighbors, and even a strong coupling is not able to change the chaotic dynamics of the orbits for each map, although the number of positive Lyapunov exponents diminishes as the coupling strength grows.

We can use the analytical result for the Lyapunov spectrum of the local case (5) to explain this result. The maximum and minimum Lyapunov exponents are λ_U and $\lambda_{min}(\epsilon)\equiv\lambda_{N/2}(\epsilon)=\ln[\beta(1-2\epsilon)]$, respectively. If $\epsilon<\tilde{\epsilon}_c=[1-(1/\beta)]/2$, we have $\lambda_{min}>0$ and all exponents are positive, giving a quite large KS-entropy density. On the other hand, even for $\epsilon\geqslant\tilde{\epsilon}_c$ ($=1/3$ for $\beta=3$) there are still typically many positive exponents, what ensures the positiveness of the KS-entropy density, that nonetheless decreases as ϵ grows. For some particular values of ϵ it is even possible to derive analytical expressions for $h(\epsilon)$, when α goes to infinity [30].

Another quantity of interest is the Lyapunov dimension D. Let p be the largest integer for which $\Sigma_{j=1}^{p}\lambda_j\geqslant 0$. Then D is defined by one of the following relations [25]:

$$D=\begin{cases} 0 & \text{if there is no such } p, \\ p+\dfrac{1}{|\lambda_{p+1}|}\displaystyle\sum_{j=1}^{p}\lambda_j & \text{if } \quad p<N, \\ N & \text{if } \quad p=N. \end{cases} \tag{9}$$

In Figure 2, we depict the Lyapunov dimension of a lattice of N piecewise linear maps with $\beta=3$ *versus* the coupling parameters α and ϵ. Weakly coupled maps, regardless of the range, have a maximum value for the Lyapunov dimension: $D_{max}=N$. It decreases sharply for a coupling strength greater than $\epsilon\approx 0.6$ to values near zero (for small α) or somewhat higher (for large α). The properties of the Lyapunov dimension are quite similar to the KS-entropy density. The decrease of Lyapunov dimension for intermediate coupling strength, in the local case, was observed for coupled logistic map lattices [34]. The very small values of D shown in Fig. 2 for a global and strong coupling suggest the existence of a low-dimensional attractor, which we will relate to a synchronized regime. On the other hand, large dimension values give us a clue of the complexity of the attractor structure in the N-dimensional state space of the coupled map lattice.

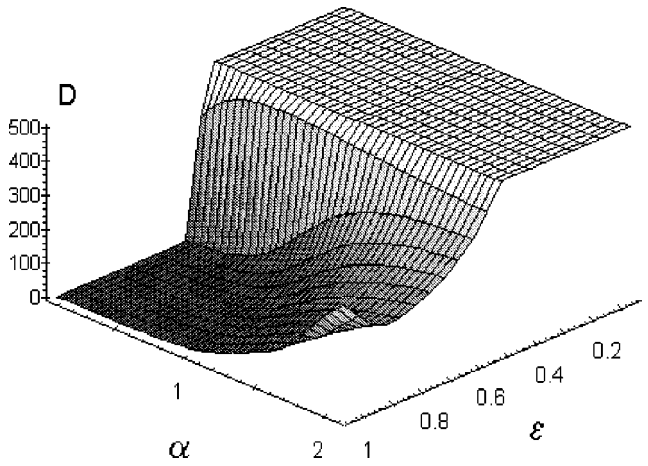

FIG. 2. Lyapunov dimension in terms of the coupling range and strength, for a lattice of $N=501$ piecewise linear maps with $\beta=3.0$, periodic boundary conditions and random initial conditions.

III. AMPLITUDE SYNCHRONIZATION

Let us now turn our attention to amplitude synchronized clusters of maps (or completely synchronized maps) for which the amplitudes $x_n^{(i)}$ are equal. For globally coupled logistic lattices these states were considered by Kaneko [8], who classified and coded the possible attractor types according to the properties exhibited by these clusters. A cluster for which all sites share a common amplitude has been called a *coherent attractor*. We will consider situations for which clusters of different sizes typically coexist with disordered lattice sites.

For a lattice of coupled maps we use as a synchronization diagnostic the dispersion of the map amplitudes with respect to their space average $\langle x\rangle_n=(1/N)\Sigma_{j=1}^{N}x_n^{(j)}$ at a given time n,

$$(\delta x)_n=\left[\frac{1}{N-1}\sum_{j=1}^{N}(x_n^{(j)}-\langle x\rangle_n)^2\right]^{1/2}. \tag{10}$$

The time evolution of the average amplitude is shown in Fig. 3 for a globally coupled lattice of N maps with $\beta=3$, after a large number of transients have decayed. The $\alpha=0$ case was taken as an example, but the gross features are the same regardless of the value adopted for the effective range parameter. For uncoupled maps [Fig. 3(a)] the average amplitude fluctuates around 1/2, which is the expected result for a uniform invariant distribution in the interval [0,1) displayed by the strongly chaotic piecewise linear maps [35].

Let $P(x_n^{(i)})$ be a probability distribution, so that $P(x_n^{(i)})dx_n^{(i)}$ gives the probability of a map iterate to fall into an interval of width $dx_n^{(i)}$, at time n. Since the distribution of iterates is uniform, $P(x_n^{(i)})=1$ for all $x_n\in[0,1)$, and we have the average $\langle x^{(i)}\rangle=\int_0^1 dx_n^{(i)}x_n^{(i)}P(x_n^{(i)})=1/2$. For coupled maps we cannot guarantee ergodicity *a priori* for the entire lattice, but if a sufficiently large number of maps remains

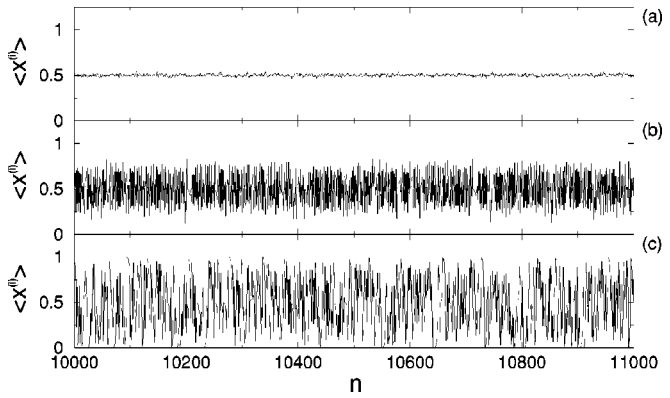

FIG. 3. Time series of the average map amplitudes for $\alpha=0.0$ and (a) $\epsilon=0.00$; (b) $\epsilon=0.60$; (c) $\epsilon=0.67$. Other parameters are the same as in the previous figures.

chaotic (or, equivalently, if h is large enough) the average amplitude is expected to be not far from 1/2 [see Fig. 3(b)], with fluctuations whose amplitudes increase with the coupling strength [Fig. 3(c)].

In Fig. 4 we show the amplitude dispersion for the same parameters as in the previous figures. For uncoupled maps [Fig. 4(a)] this quantity is approximately constant at 0.29, which is expected from a uniform distribution of iterates since in this case $(\delta x)_n=[\int_0^1 dx_n^{(i)}P(x_n^{(i)})(x_n^{(i)}-\langle x^{(i)}\rangle)^2]^{1/2}=1/\sqrt{12}$. For nonzero coupling the maps pass from a nonsynchronized, due to the oscillatory behavior of the dispersion [Fig. 4(b)], to a completely synchronized state [Fig. 4(c)], characterized by no dispersion at all with respect to the corresponding space average. The fact that the averages themselves are oscillating chaotically [Fig. 3(c)] suggests that the chaotic maps are completely synchronized in amplitude: $x_n^{(1)}=x_n^{(2)}=\cdots=x_n^{(N)}\equiv x_n$, thus defining a one-dimensional synchronization manifold $\mathcal{M}$ embedded in the N-dimensional state space [4]. If the Lyapunov exponent related to the direction defined by $\mathcal{M}$ is positive (negative), the completely synchronized state is chaotic (periodic). There are also $N-1$ mutually orthogonal directions transversal to $\mathcal{M}$.

A completely synchronized state is actually a possible solution for a lattice with power-law coupling. This result follows directly from substituting the common amplitude of the sites, x_n, into Eq. (1), which gives

$$x_{n+1}=(1-\epsilon)f(x_n)+\frac{\epsilon}{\eta(\alpha)}\sum_{j=1}^{N'}\frac{2f(x_n)}{j^\alpha}=f(x_n),$$

which reflects a symmetry inherent to a large class of coupling forms [36], and implies that the synchronization manifold $\mathcal{M}$ is invariant under the application of the map $f(x)$. An initial condition for the lattice, $x_0^{(i)}$, that belongs to $\mathcal{M}$ will generate subsequent spatiotemporal patterns $x_n^{(i)}$ that remain in $\mathcal{M}$ for all times n.

However, the fact that a completely synchronized state is possible does not necessarily imply that it will be actually observed. If $\mathcal{M}$ is transversally unstable such a completely synchronized state will not be achieved by typical spatiotemporal patterns. A necessary, albeit not sufficient, condition for existence of a completely synchronized state is that all the $(N-1)$ Lyapunov exponents corresponding to the directions transversal to $\mathcal{M}$ be negative. If the synchronized state is chaotic the KS-entropy density goes to zero with an increasing lattice size.

These arguments are supported by another numerical diagnostic of amplitude synchronization: the complex order parameter introduced by Kuramoto [28], and here adapted for coupled map lattices as [19]

$$z_n=R_n\exp(2\pi i\varphi_n)\equiv\frac{1}{N}\sum_{j=1}^{N}\exp(2\pi i x_n^{(j)}), \qquad (11)$$

where R_n and φ_n are the amplitude and angle, respectively, of a centroid phase vector for a one-dimensional lattice with periodic boundary conditions. Figure 5 shows the time evolution of the order parameter magnitude for the same parameters as in the previous figures.

For uncoupled maps, we expect a pattern in which the site amplitudes $x_n^{(j)}$ are so spatially uncorrelated that they may be considered essentially as random variables. In this case the order parameter $z_n=\langle e^{2\pi i x_n^{(j)}}\rangle_j$ nearly vanishes for all times. This is indeed observed for the uncoupled case depicted in Fig. 5(a), in which the order parameter magnitude exhibits small oscillations about a value close to zero. In a completely

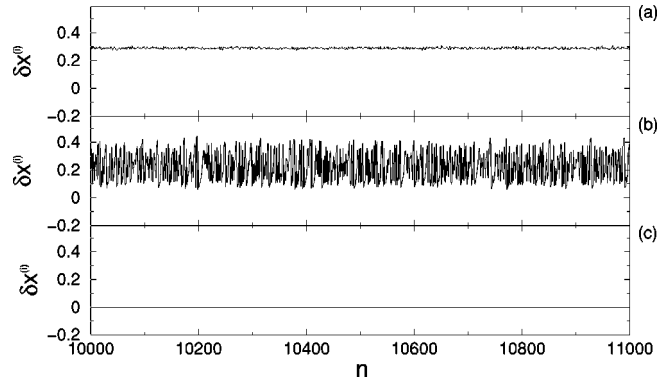

FIG. 4. Time series of the amplitude dispersion for $\alpha=0.0$ and (a) $\epsilon=0.00$; (b) $\epsilon=0.60$; (c) $\epsilon=0.67$.

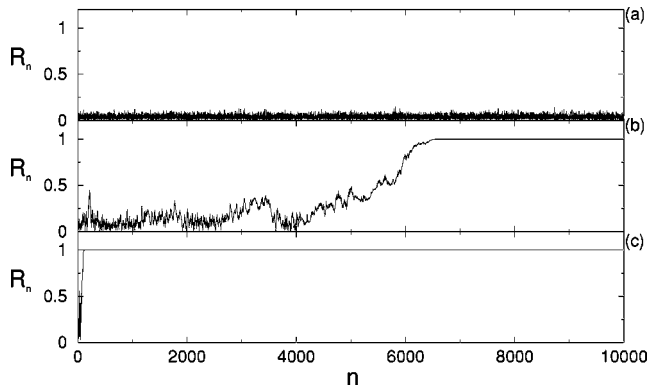

FIG. 5. Time series of the order parameter magnitude for $\alpha=0.0$ and (a) $\epsilon=0.00$; (b) $\epsilon=0.60$; (c) $\epsilon=0.67$.

synchronized state, like that depicted in Fig. 5(c), the order parameter magnitude rapidly grows to unity, indicating the coherent superposition of the phase vectors for all sites with the same (chaotic) amplitudes at each time. The synchronization transient in the case of Fig. 5(c) is very short, but may also have an arbitrarily long duration, as illustrated by Fig. 5(b). There is a transition to an amplitude-synchronized state as the coupling range varies from global to local, such as those previously found in chains of discrete and continuous-time oscillators [18–20], and even in kinetic Ising models with a power-law form of interaction between spins [37].

The amplitude-synchronized state may present intermittent bursts of nonsynchronized behavior when the effective range parameter assumes moderately large values, where the above-mentioned phase transition occurs. This intermittency is revealed, in a time series of the amplitude dispersion, as a sequence of the laminar phases with different durations interrupted by bursts. We can understand the existence of this bursting by considering the invariant manifold $\mathcal{M}$ corresponding to a completely synchronized state. Suppose for simplicity that there is only one direction transversal to $\mathcal{M}$, and that λ_T is the Lyapunov exponent related to this direction, for initial conditions belonging to $\mathcal{M}$, and such that if $\lambda_T<0$ the synchronized state is transversally stable. In the case of more than one transversal direction one should use the master stability function technique developed by Pecora and Carroll [38] in order to verify the stability of $\mathcal{M}$.

It is useful to consider also the finite-time transversal Lyapunov exponent $\lambda_T(n)$, which is obtained by taking a short time interval of length *n*. The Lyapunov exponent λ_T is the infinite-time limit of $\lambda_T(n)$ and it is independent of the initial condition, contrary to $\lambda_T(n)$ that typically depends on it [35]. The finite-time exponents typically have a statistical distribution whose mean is λ_T, and with fluctuations that may have positive as well negative values. Let λ_T be slightly higher than zero, hence if an initial condition $x_0^{(i)}$ for the lattice starts near but off the synchronization manifold $\mathcal{M}$, it will initially wander nearby $\mathcal{M}$ resulting in the laminar intervals, but the pattern eventually moves far away from $\mathcal{M}$ [39]. However, because of the fluctuations inherent to the finite-time transversal exponents there are intervals for which $\lambda_T(n)<0$ and the lattice pattern approaches $\mathcal{M}$, forming the intermittent bursts before returning to a new laminar state. This effect has been studied in the context of the so-called *on-off intermittency* [40,41]. For more than one transversal direction this mechanism still applies [5].

The average duration of these synchronization laminar phases was found to obey a power-law dependence with the difference between the range parameter and a critical value $\alpha_c \approx 0.486\,875$, in the form $\langle \tau \rangle = \tilde{K}(\alpha-\alpha_c)^{\gamma}$, where the exponent was found to be $\gamma = 0.202\,47$ (Fig. 6). When $\alpha \to \alpha_c^+$ the average laminar duration goes to infinity and eventually results in a steady synchronized state for $\alpha \leqslant \alpha_c$. We remark that this critical value of α for a steady synchronizated state is close to the value after which the KS entropy begins to increase, when $\epsilon = 1$ [see Fig. 1]. This corroborates the already mentioned fact that for a completely synchronized state the KS-entropy density either vanishes or is extremely small ($\sim 1/N$) [42].

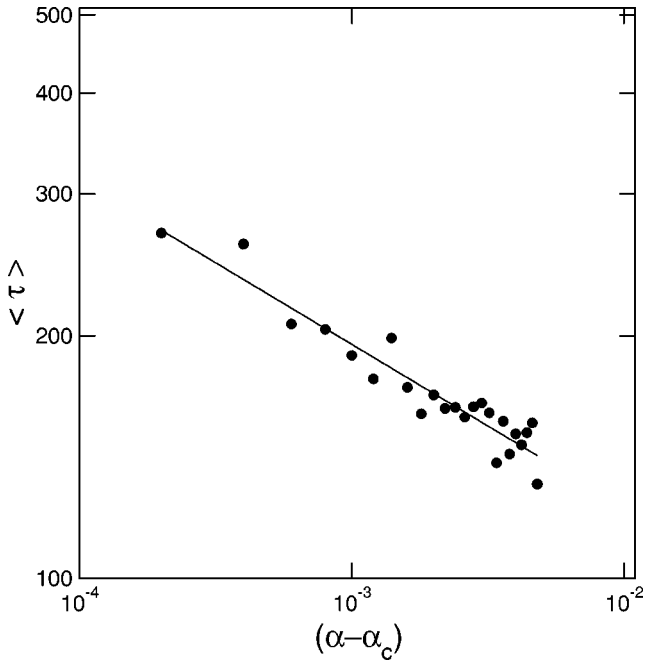

FIG. 6. Average duration of synchronization laminar intervals for $\epsilon = 1.0$ as a function of $\alpha - \alpha_c$ for $\alpha_c = 0.486\,875$. Five initial conditions were used for computing the average. The solid line is a power-law fit.

The results of Fig. 5 suggest that it is useful to consider the mean value of the space-averaged order parameter magnitude

$$\langle \overline{R} \rangle = \lim_{n\to\infty} \frac{1}{nN} \sum_{j=1}^{N} \sum_{m=0}^{n} R_m^{(j)}, \tag{12}$$

and Fig. 7 shows its dependence with the coupling strength ϵ and range α. Considering first the ''mean-field'' case ($\alpha = 0$) for weak coupling the mean order parameter is very small, indicating absence of synchronization, a situation that changes with increasing ϵ to a completely synchronized state. For nearest-neighbor coupling, however, the mean order parameter remains small for all the considered values of

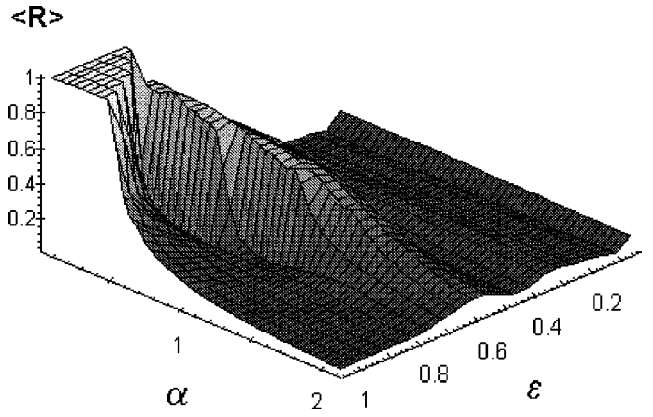

FIG. 7. Mean value of the space-averaged order parameter magnitude in terms of the coupling range and strength, for a lattice of $N = 501$ piecewise linear maps with $\beta = 3.0$.

ϵ, indicating that a locally coupled lattice does not exhibit amplitude synchronization at all, irrespective of how strong ϵ is [11]. For intermediate effective range we do not find a simple interpolation between these two limiting cases, since for moderately strong coupling there is a bump of higher values of $\langle \overline{R} \rangle$, what implies the existence of a number of coexisting amplitude synchronization clusters. However, even this bump is smoothed out as α increases.

IV. PHASE SYNCHRONIZATION

There are many situations of physical interest in which two or more continuous-time oscillators may have different amplitudes, even in a chaotic regime, but with a *phase coherence*. The oscillator phase can be defined in various ways for continuous-time systems, the simplest one being a geometrical phase for a bounded attractor [43,44]. For coupled map lattices, an operational definition of phase-synchronized states has been proposed by Hu and Liu [29], as those states showing local maxima or minima for their amplitudes at the same time. The direction phase is provided by the direction of two sequential iterations of the coupled maps [45]. A quantitative definition of phase for a given lattice site $x_n^{(j)}$ at a time n is thus

$$P_n^{(j)} = \begin{cases} 1 & \text{if } x_n^{(j)}/x_{n-1}^{(j)} > 1, \\ 0 & \text{otherwise} \end{cases} \tag{13}$$

in such a way that a phase-synchronized cluster is a reunion of adjacent sites with the same value of $P_n^{(j)}$.

Figure 8(a) shows the overlap of amplitude-site profiles, for a hundred successive times and after a large number of transients have decayed, for a lattice of strongly coupled maps with $\beta = 3.0$, in the intermediate range situation. Since the KS-entropy density for this lattice is $h \approx 2.2 \times 10^{-3}$, it is expected that many of these maps are behaving chaotically. In order to allow for a better visualization of the local maxima and minima, in Fig. 8(b) we depict only three sequential profiles, where the arrows show the phase directions. On the basis of the previous definition we can say that at times $n = 2972$ and 2973 all sites in Fig. 8 are phase synchronized, whereas at $n = 2974$ this occurs just for a fraction of them.

Let us denote by $\mathcal{N}_n^{(0)} = \Sigma_{j=1}^{N}(P_n^{(j)} = 0)$ and $\mathcal{N}_n^{(1)} = \Sigma_{j=1}^{N}(P_n^{(j)} = 1)$ the number of lattice sites at a given time with phases equal to 0 and 1, respectively. We define a phase-synchronized ratio ρ_n as [45]

$$\rho_n \equiv \frac{1}{N} \max(\mathcal{N}_n^{(0)}, \mathcal{N}_n^{(1)}) \tag{14}$$

in such a way that, if the phases of all lattice sites flip randomly between 0 and 1, its ratio would approach a constant value, whereas if $\rho = 1$ all lattice sites are in phase. The minimum value for this ratio is $\rho = 1/2$, a situation in which half of the sites have a zero phase.

As the lattice pattern evolves with time, this ratio varies in an intermittent fashion, as illustrated by Fig. 9, where the parameters are the same as in the previous figure. The phase

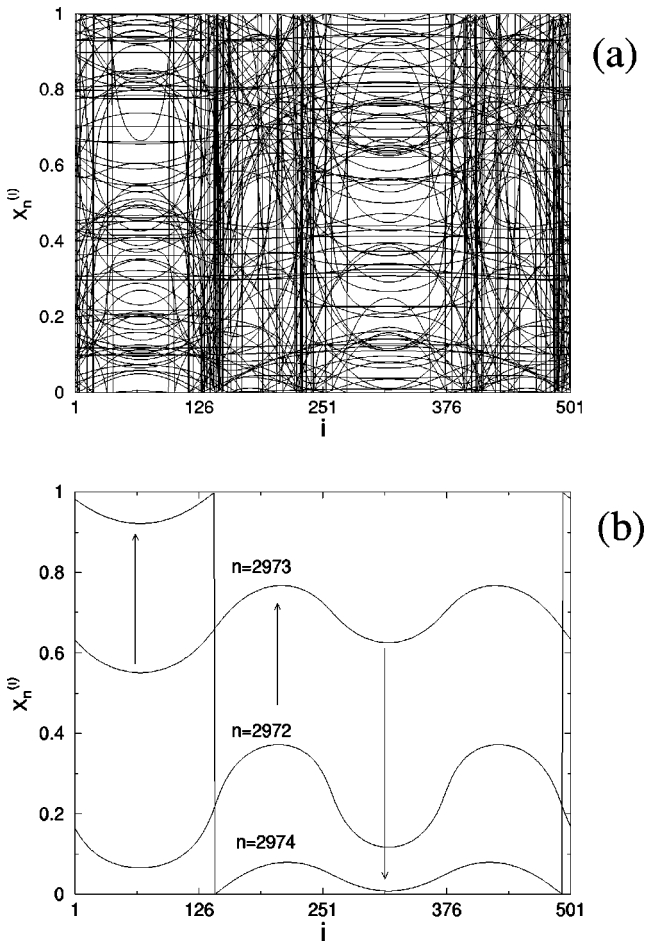

FIG. 8. Overlap of (a) 100, and (b) three space-amplitude plots, after 2900 transients, for a lattice of $N = 501$ maps with $\alpha = 0.49$, and $\epsilon = 1.0$. The arrows in (b) indicate the phase direction.

synchronization ratio has laminar phases at 1.0 with irregular bursts, some of them approaching the lower bound at $\rho = 1/2$, indicating an intermittent behavior very similar to that described in the preceding section for amplitude synchroni-

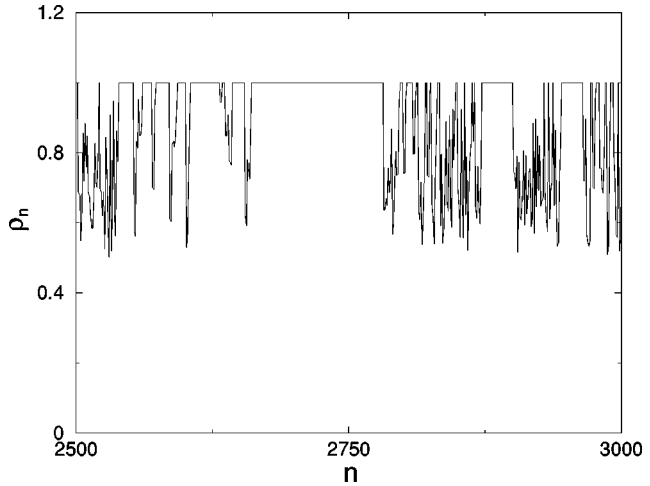

FIG. 9. Time series of the phase-synchronization ratio for $N = 501$, $\alpha = 0.49$, and $\epsilon = 1.0$.

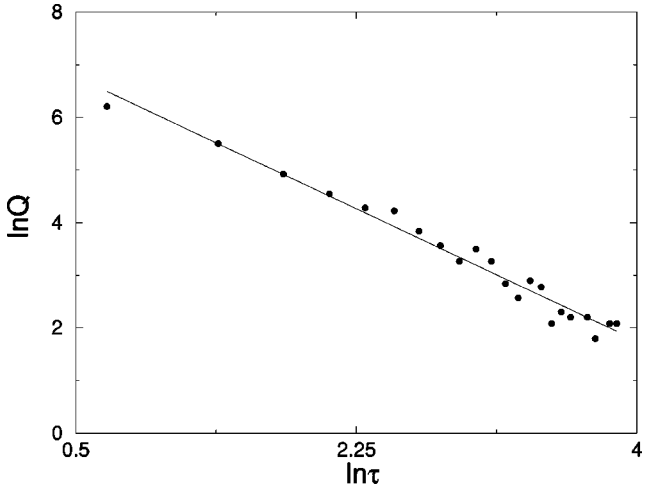

FIG. 10. Number of phase-synchronization laminar intervals *versus* laminar lengths for $N=501$, $\alpha=0.49$, and $\epsilon=1.0$. There were considered 42 000 iterations and 2000 transients were discarded. The solid line is a power-law fit.

zation. The average duration of the laminar intervals scales with the range parameter in a power-law fashion, just like that depicted in Fig. 6 and with the same exponent, showing that both share the same mechanism for bursting.

The number of phase-synchronization laminar intervals also depends on the interval lengths according to another power-law distribution (cf. Fig. 10) $Q(\tau)=\kappa\tau^{-\sigma}$, with a slope fit $\sigma\approx 1.43$. We remark that σ is close to the slope 3/2 theoretically predicted for the distribution of laminar intervals characteristic of on-off intermittency [40]. Hence we have numerical evidence that the phase- and amplitude-synchronization intermittency is actually a manifestation of on-off intermittency, in which the invariant manifold of interest is the synchronization manifold $\mathcal{M}$. We have also found that σ does not depend in a significant way on the coupling strength ϵ, as illustrated by Fig. 11(a), where α was kept constant and ϵ was varied between 0.965 and 0.980. Outside this range the regime where phase synchronization is interrupted by bursts no longer exists. Similarly, for constant ϵ the power-law exponent σ also does not change appreciably with the range parameter α, as can be seen in Fig. 11(b), in which the horizontal axis represents the difference $\alpha-\alpha_c$ for $\alpha_c=0.486\,875$ (see also Fig. 6).

There is also a transition between phase-synchronized and nonsynchronized states, which can be evidenced by analyzing the dependence on the coupling parameters of the mean ratio of phase-synchronized states $\overline{\rho}(\epsilon,\alpha)=\lim_{n\to\infty}(1/n)\Sigma_{m=0}^{n}\rho_m$, as depicted by Fig. 12 which is very similar to Fig. 7, where the mean order parameter was plotted against the same variables. The shapes of both diagrams are basically the same for small and large effective ranges, even with the bump characteristic of moderate coupling. This means that, at least for the parameter ranges considered in this work, amplitude synchronization implies phase synchronization.

V. CONCLUSIONS

Spatiotemporal chaos and synchronization are collective phenomena typically displayed by coupled map lattices. The

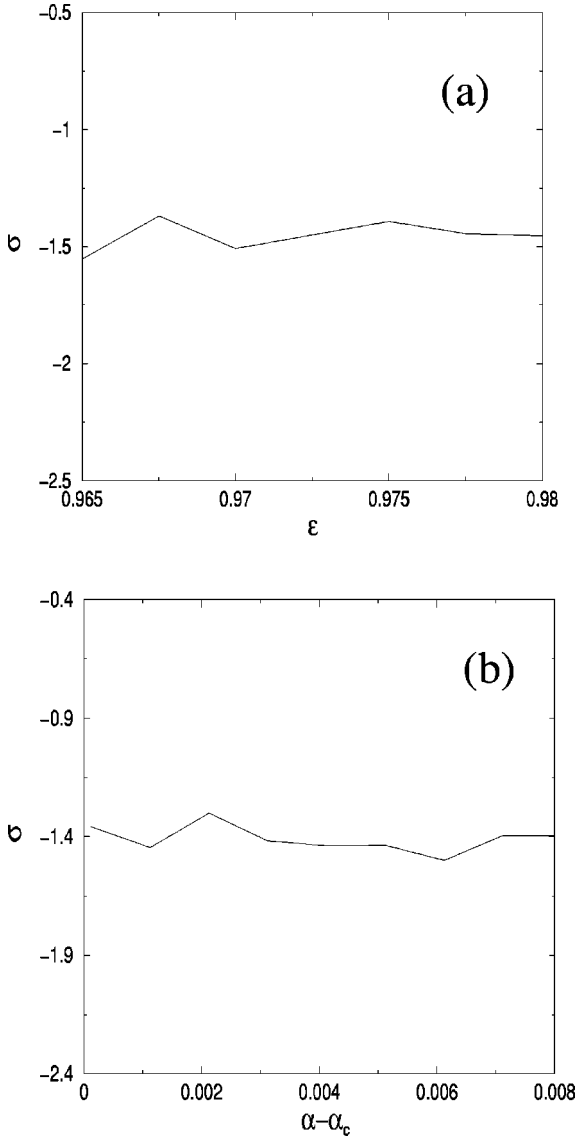

FIG. 11. Exponent of the power-law distribution of phase-synchronization laminar regions *versus*: (a) ϵ, for $\alpha=0.47$; (b) $\alpha-\alpha_c$, with $\epsilon=1.0$, and $\alpha_c=0.486\,875$.

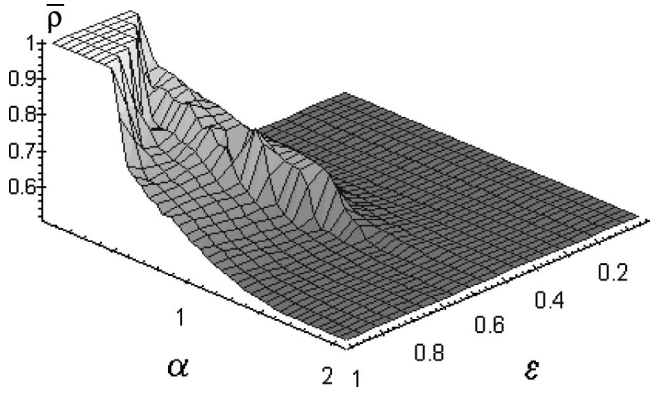

FIG. 12. Mean value of the phase-synchronization ratio in terms of the coupling range and strength for $N=501$ and $\beta=3.0$.

relation between them, however, is a complex issue since there are many forms of synchronization of periodic and chaotic dynamics. We have chosen to study lattices of piecewise linear maps because they exhibit, when uncoupled, strong chaos with a uniform invariant distribution. In addition to this fact, piecewise linear maps have constant slope and the Lyapunov spectrum may be studied in detail. Quantities of interest in this study are the KS-entropy density and the Lyapunov dimension.

The coupling properties play a fundamental role on the lattice dynamics. We have used a coupling prescription that makes possible to pass continuously from a global to a local coupling scheme. Our numerical results show that for short effective range the diffusive effect due to coupling is not sufficient to surpass the intrinsic randomness of the maps. On the other hand, for long coupling range the KS-entropy behavior indicates a transition from weak to strong chaos, as the coupling strength evolves past a critical value.

Complete synchronization is characterized with the help of the amplitude dispersion and a complex-valued order parameter, and we analyze the time evolution of its magnitude. We found that, for short effective range the lattice never synchronizes, irrespective of its coupling strength. As the effective range becomes longer, a moderate coupling strength is enough to make a number of lattice sites become more coherent, although not completely synchronized. For strong coupling, however, there is complete synchronization as we approach the globally coupled case. In the latter case, there is a transition very similar to that exhibited by the KS entropy.

We have used a phase definition for coupled map lattices based on the directional properties of the maximum map amplitudes, in order to investigate to what extent we can observe phase synchronization. The phases can assume only two values, and their ratio is a quantity similar to the order parameter. Accordingly, the dependence of this ratio is very similar to the complex order parameter, such that amplitude synchronization implies phase synchronization for this system. For intermediate ranges the time evolution of this phase-synchronization ratio has laminar regions alternated with intermittent bursts of nonsynchronization, which were found to obey a power-law dependence within the effective range. This fact was also observed for amplitude synchronization and is related to the properties of the infinite- and finite-time Lyapunov exponents in the directions transversal to the synchronization manifold.

The distribution of the average duration of interburst laminar intervals scales with an exponent close to 3/2, suggesting that it is a manifestation of on-off intermittency, for there is an invariant synchronization manifold embedded in the high-dimensional phase space of the coupled map lattice, and with the necessary stability properties with respect to displacements in directions transversal to this manifold.

ACKNOWLEDGMENTS

This work was made possible by partial financial support from the following Brazilian government agencies: CNPq, CAPES, Fundação Araucária (Paraná), and UFPR/FUNPAR.

[1] J. P. Crutchfield and K. Kaneko, in *Directions in Chaos*, edited by H.-B. Lin (World Scientific, Singapore, 1987), Vol. 1.
[2] K. Kaneko, in *Theory and Applications of Coupled Map Lattices*, edited by K. Kaneko (Wiley, Chichester, 1993).
[3] L.M. Pecora, T.L. Carroll, G.A. Johnson, D.J. Mar, and J.F. Heagy, Chaos **7**, 520 (1997), and references therein.
[4] L. Pecora and T. Carroll, Phys. Rev. Lett. **64**, 821 (1990).
[5] R. Brown and N. Rulkov, Chaos **7**, 395 (1997).
[6] K. Kaneko, Physica D **34**, 1 (1989).
[7] K. Kaneko, Physica D **23**, 436 (1986).
[8] K. Kaneko, Physica D **41**, 137 (1990).
[9] T. Shimada and K. Kikuchi, Phys. Rev. E **62**, 3489 (2000).
[10] H. Nozawa, Chaos **2**, 377 (1992); S. Ishii and M. Sato, Physica D **121**, 344 (1998).
[11] P.M. Gade and C.-K. Hu, Phys. Rev. E **60**, 4966 (1999).
[12] Y. Kuramoto and H. Nakao, Physica D **103**, 294 (1997).
[13] Y. Kuramoto, D. Battogtokh, and H. Nakao, Phys. Rev. Lett. **81**, 3543 (1998).
[14] S. Raghavachari and J.A. Glazier, Phys. Rev. Lett. **74**, 3297 (1995).
[15] R. Kozma, Phys. Lett. A **244**, 85 (1998).
[16] D.J. Watts and S.H. Strogatz, Nature (London) **393**, 440 (1998); S.H. Strogatz, *ibid.* **410**, 268 (2001).
[17] J.L. Rogers and L.T. Wille, Phys. Rev. E **54**, R2193 (1996).
[18] R.L. Viana and A.M. Batista, Chaos, Solitons Fractals **9**, 1931 (1998).
[19] S.E. de S. Pinto and R.L. Viana, Phys. Rev. E **61**, 5154 (2000).
[20] S.E. de S. Pinto, S.R. Lopes, and R.L. Viana, Physica A **303**, 339 (2002).
[21] M. Bahiana and M.S.O. Massunaga, Phys. Rev. E **52**, 321 (1995).
[22] S. Isola, A. Politi, S. Ruffo, and A. Torcini, Phys. Lett. A **143**, 365 (1990).
[23] D. Ruelle, *Chaotic Evolution and Strange Attractors* (Cambridge University Press, Cambridge, 1989).
[24] R. Carretero-González, S. Ørstavik, J. Huke, D.S. Broomhead, and J. Stark, Chaos **9**, 466 (1999).
[25] K. A. Alligood, T. Sauer, and J. A. Yorke, *Chaos: An Introduction to Dynamical Systems* (Springer, New York, 1997).
[26] H. Shibata, Physica A **292**, 182 (2001).
[27] A.M. Batista and R.L. Viana, Phys. Lett. A **286**, 134 (2001).
[28] Y. Kuramoto, *Chemical Oscillations, Waves, and Turbulence* (Springer-Verlag, Berlin, 1984).
[29] B. Hu and Z. Liu, Phys. Rev. E **62**, 2114 (2000).
[30] A. M. Batista and R. L. Viana, Physica A (to be published).
[31] Y.B. Pesin, Russ. Math. Surveys **32**, 55 (1977).
[32] D. Ruelle, Bol. Soc. Bras. Mat. **9**, 83 (1978).
[33] J. Bricmont and A. Kupiainen, Physica D **103**, 18 (1997).
[34] C. Boldrighini, L.A. Bunimovich, G. Cosimi, S. Frigio, and A. Pellegrinotti, J. Stat. Phys. **102**, 1271 (2001).
[35] E. Ott, *Chaos in Dynamical Systems* (Cambridge University Press, Cambridge, 1994).

[36] Y.-C. Lai and C. Grebogi, Phys. Rev. Lett. **82**, 4803 (1999).
[37] M.E. Fisher, S. Ma, and B.G. Nickel, Phys. Rev. Lett. **29**, 917 (1972); M.E. Fisher, Rev. Mod. Phys. **46**, 597 (1974).
[38] L.M. Pecora and T.L. Carroll, Phys. Rev. Lett. **80**, 2109 (1998).
[39] S.C. Venkataramani, T.M. Antonsen, Jr., E. Ott, and J.C. Sommerer, Phys. Lett. A **207**, 173 (1995).
[40] N. Platt, E.A. Spiegel, and C. Tresser, Phys. Rev. Lett. **70**, 279 (1993); J.F. Heagy, N. Platt, and S.M. Hammel, Phys. Rev. E **49**, 1140 (1994).
[41] C.-M. Kim, Phys. Rev. E **56**, 3697 (1997).
[42] L. Baroni, R. Livi, and A. Torcini, Phys. Rev. E **63**, 036226 (2001).
[43] G.V. Osipov, A.S. Pikovsky, M.G. Rosenblum, and J. Kurths, Phys. Rev. E **55**, 2353 (1997).
[44] A.S. Pikovsky, M.G. Rosemblum, G.V. Osipov, and J. Kurths, Physica D **104**, 219 (1997).
[45] W. Wang, Z. Liu, and B. Hu, Phys. Rev. Lett. **84**, 2610 (2000).